Spring 2017

# The Relationship Among Suture Complexity, Shell Form, and Stratigraphic Formation In Ammonites Of The Western Interior Seaway

Darrah Jorgensen
*Fort Hays State University*, ddjorgensen@mail.fhsu.edu

THE RELATIONSHIP AMONG SUTURE COMPLEXITY, SHELL FORM,

AND STRATIGRAPHIC FORMATION IN AMMONITES OF THE

WESTERN INTERIOR SEAWAY

being

A Thesis Presented to the Graduate Faculty

of the Fort Hays State University in

Partial Fulfillment of the Requirements for

the Degree of Master of Science

by

Darrah Jorgensen

B.S., South Dakota School of Mines and Technology

Date___________________ Approved_______________________________________

Major Professor

Approved_______________________________________

Chair, Graduate Council

GRADUATE COMMITTEE APPROVAL

The graduate committee of Darrah Jorgensen approves this thesis as meeting partial fulfillment of the requirements for the Degree of Master of Science.

Approved_________________________________
Chair, Graduate Committee

Approved_________________________________
Committee Member

Approved_________________________________
Committee Member

Date_________________________

ABSTRACT

Throughout ammonite evolution, shell suture patterns grew increasingly more complex, but the purpose of these sutures has long been debated. One hypothesis is that suture complexity is related to the structural integrity of the shell under pressure. To test this hypothesis, suture complexity was compared to shell form and stratigraphic formation to determine if there were significant differences in suture complexity, as a proxy for structural integrity, among shell forms or stratigraphic formations. Highly complex sutures might have allowed for the tightly coiled form of many ammonites, an advantage compared to less coiled forms because the pressure is distributed over more points on the shell. If this is the case, coiled forms should have more complex suture patterns. Suture pattern complexities of coiled, straight, and heteromorphic ammonite shell forms from the Pierre, Carlile, Greenhorn, Graneros, and Mowry shales were quantified using box-counting fractal analysis. Results indicate there is a significant difference in the median suture complexity among the defined shell forms ($H = 27.9$, $df = 2$, $p < 0.001$). A Kruskal-Wallis multiple comparisons test confirms there is a significant difference in median suture complexity between coiled and heteromorphic shell forms ($p < 0.03$), and a significant difference in median suture complexity between heteromorphic and straight shell forms ($p < 0.03$). However, there is no significant difference in median suture complexity between coiled and straight shell forms ($p > 0.03$). The most complex suture patterns are typically found in tightly coiled shells, possibly adding structural support as the coiled form evolved. Most of the straight shell forms examined in this project evolved from coiled forms and perhaps retained highly complex sutures to protect against hydrostatic pressure. On the other hand, heteromorphic shell forms may have significantly reduced their suture complexity to loosen the coil of their shell. However, these forms did not require suture patterns as complex as the straight shell forms because the partially coiled shell would have provided more protection against hydrostatic pressure than the straight shell. Results also show no significant difference in median suture complexities among formations ($H = 5.24$, $df = 4$, $p = 0.264$), suggesting that there is no significant change in median suture complexity over time.

## ACKNOWLEDGMENTS

This project has been made possible with the help, advice, and support of many individuals. Thank you to the Denver Museum of Nature of Science, Fort Hays State University's Sternberg Museum of Natural History, University of Kansas Biodiversity Institute and Natural History Museum, South Dakota School of Mines and Technology Museum of Geology, University of Colorado Museum of Natural History, United States Geological Survey, and the University of Texas Memorial Museum for allowing access to their fossil collections. I would like to thank the members of my thesis committee: Dr. Laura Wilson, Dr. Robert Channell, and Dr. Ken Neuhauser. They helped me through many unforeseen difficulties. Finally, I would like to thank Dylan Steffen for his unfailing support throughout my thesis neurosis.

TABLE OF CONTENTS

LIST OF TABLES

LIST OF FIGURES

LIST OF APPENDICES

# INTRODUCTION

The clade Ammonoidea encompasses a group of extinct molluscan cephalopods that thrived in the Late Cretaceous Western Interior Seaway. Ammonoidea includes the ammonites and their relatives – the goniatites and ceratites. This clade is closely related to living nautiloids. However, ammonites have more complex septa than nautiloids (Dzik, 1984). Septa are shallow, concave walls that divide the ammonoid shell into chambers. Ammonite septa contain folds that radiate outward from the center of the shell and become more tightly folded as they merge with the shell's exterior wall (Monks and Palmer, 2002). The pattern in which the septa join with the shell wall forms the shell's suture pattern (Li et al., 2011). Suture patterns have changed through time, and so are used for taxonomic identification (Westermann, 1996; Wippich and Lehmann, 2004).

The function of sutures in ammonite shells has been widely debated among researchers, and several hypotheses have been proposed. The most widely accepted hypotheses consider complex sutures as a component in resisting stress caused by hydrostatic pressure (Daniel et al., 1997; Boletzky, 1999; Olóriz et al., 2002). Complex sutures may have evolved as a mechanism not only to resist hydrostatic pressure, but also to aid the formation of the different shell forms by supporting the coiled phragmocone (Pérez-Claro et al., 1997).

Jacobs (1990) suggests that different suture patterns in *Baculites* – a straight-shelled ammonite – were caused by differences in the environments in which the organisms lived. Complex suture patterns in *Baculites* might have provided increased structural support against compressional forces when the organisms were adjusting to changing water pressures as they moved vertically in the water column. The complex suture patterns allowed for a thickening of the shell, which would have acted as buttresses by giving the shell the ability to resist shattering from pressure.

Pérez-Claro et al. (1997) analyzed suture patterns and whorls resulting from coiling, and suggested that sutures increased shell tensile strength rather than compressional strength. The authors concluded that complex sutures help strengthen the shell and increase its structural integrity as it bends.

Other research indicates that complex sutures give no functional advantage to the organism (Boyajian and Lutz, 1992). Olóriz et al. (2002) reexamined the functional significance of septa by analyzing the suture complexity of ammonoids colonizing deep habitats in the Late Jurassic and found no trend among suture complexities and the whorl, coiling, or shell shape.

Previous research has only examined complexity in a single shell form. The relationship among suture complexity, shell form, and stratigraphic formation has not previously been examined. Western Interior Seaway ammonites exhibited a wide range of straight, coiled, and heteromorphic (semi-coiled) shell forms. The ancestral ammonite shell form is a long, straight shell such as the orthocone (Figure 1). Most ammonites, however, had coiled shells, which evolved in the Devonian from the ancestral straight-shell form (Monks and Palmer, 2002). Some ammonite lineages – such as *Baculites* – secondarily evolved a straight shell from coiled shells.

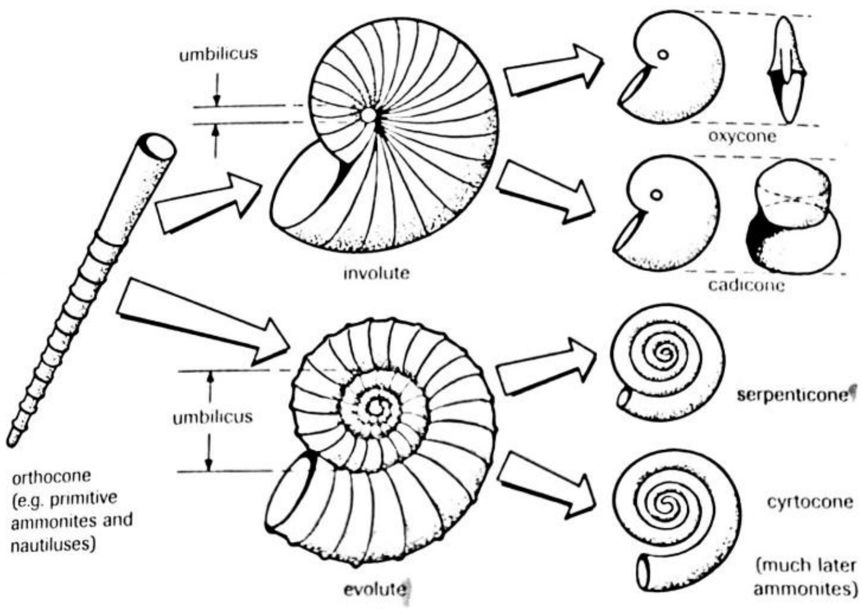


Figure 1: **Evolution of Ammonite Shells from Basal Straight Form.** The ancestral straight shell form (orthocone) evolved into the coiled shell form, splitting into two varieties. These forms split again into a variety of forms, with the evolute shell secondarily uncoiling. Figure from Monks and Palmer, 2002.

While Ammonitida exhibits several types of suture patterns (Figure 2), ammonitic sutures are prevalent in the shells of ammonites found in Western Interior Seaway deposits. Ammonitic sutures typically have rounded lobes and saddles that are subdivided or fluted (Figure 2). This suture pattern is found in both straight and coiled shell forms, though it is not clear if and how suture patterns relate to shell form. The primary purpose of this study is to examine the relationship between suture complexity and shell form in

Cretaceous ammonites. The suture patterns of coiled, straight, and heteromorphic ammonite shell forms from five shales of the Western Interior Seaway were quantified using box-counting fractal analysis to determine if there is a significant difference in suture complexity through the Cretaceous among shell forms. In this study, suture complexity is used as a proxy for structural integrity. If complex suture patterns provide increased shell strength (*sensu* Pérez-Claro et al., 1997), then coiled ammonites should have more complex suture patterns due to the increased complexity of the shell's shape.

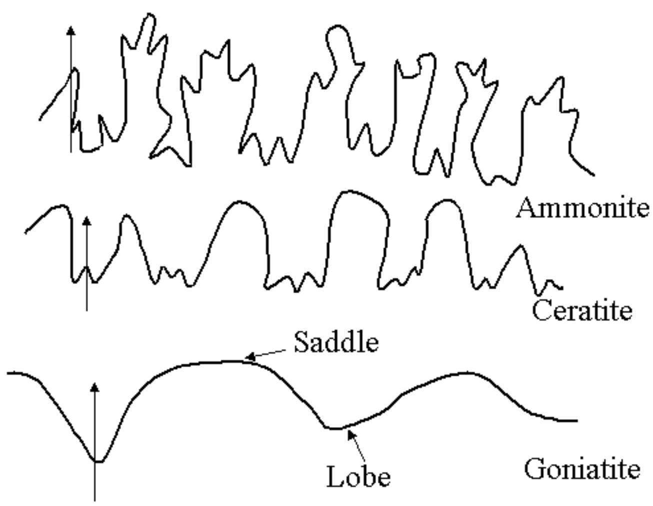


Figure 2: **Varieties of Suture Complexities found in Ammonoidea**: The three common types of suture patterns in Ammonoidea. The most complex fluting is found within ammonitic sutures. Figure from Pérez-Claro et al., 1997.

## Quantifying Complexity

It is necessary that researchers use a consistent method for defining complexity during a study, but determining the best method of defining suture pattern complexity has been debated among researchers as often as suture function itself (Jacobs, 1990; Daniel et al, 1997; Allen, 2006). This is significant because utilizing different complexity measures could affect the results of the study. Historically, there have been three methods used to define suture pattern complexity: the Fourier method, GIS, and fractal analysis.

Fourier waveform analysis is primarily used to represent complex shapes as components of sine waves. A Short-time Fourier transform (STFT) divides a long-time signal into shorter segments of equal length and applies a Fourier transform separately on each shorter segment (Allen, 1977). The STFT is usually plotted as a function of time. The Fourier method determines whether components close together are separate, or if there is a change in frequencies. On ammonites, a STFT examines the suture line to find variance, and creates a function that best fits the smoothed reproduction of each suture pattern (Allen, 2006).

One of the limitations of the Fourier method is that it uses a fixed resolution or window width, and the width of the window is related to how the signal is represented. A wide window gives greater frequency resolution, but poor time resolution. A narrower window gives greater time resolution, but poor frequency resolution. Maximizing one will minimize the other, lowering the power of the analysis.

Manship (2004) developed a method that uses ArcGIS™ to create templates to aid in identification of unknown ammonite specimens by mapping the suture complexity of ammonites. In her study, suture complexity showed little variability among suture forms and among species. Yacobucci and Manship (2011) employed similar methods using GIS to quantify the suture complexity by determining distances between points on the suture. The templates were compared to unknown specimens to identify them (Yacobucci and Manship, 2011).

GIS methods are accurate in the placement of points and user-friendly. However, there is subjectivity in the method, as the points are placed manually, possibly leading to error in point positioning. Despite its utility in identifying specimens based on suture pattern, the GIS method cannot quantify suture complexity.

Several types of fractal analyses have been performed to quantify ammonite suture complexity. Lutz and Boyajian (1995) calculated the fractal dimensions of several ammonoid genera. A fractal dimension is a ratio providing an index of complexity by comparing how details in a pattern change with scale. This technique is useful for quantifying complicated geometric forms in which the details at small scales are more important than the overall form at larger scales. These fractal forms are defined as self-similar and irregular (Vicsek, 1992). Because ammonitic suture patterns are self-similar and bend irregularly, with the irregularity of the suture changing based on how it is oriented when measured, the complexity of these patterns can be quantified well using fractal analysis.

*Institutional abbreviations* – **DMNS**, Denver Museum of Nature and Science, Denver, Colorado, U.S.A.; **FHSM**, Fort Hays State University Sternberg Museum of Natural History, Hays, Kansas, U.S.A.; **KUIP**, Invertebrate Paleontology, University of Kansas Biodiversity Institute and Natural History Museum, Lawrence, Kansas, U.S.A.; **SDSM**, South Dakota School of Mines and Technology Museum of Geology, Rapid City, South Dakota, U.S.A.; **UCM**, University of Colorado Museum of Natural History, Boulder, Colorado, U.S.A.; **USGS,** United States Geological Society Core Research Center, Denver, Colorado, U.S.A.; **UT**, University of Texas Non-Vertebrate Paleontology Lab, Austin, Texas, U.S.A.; and **YPMIP**, Yale Peabody Museum of Natural History, New Haven, Connecticut, U.S.A.

## MATERIALS & METHODS

### Study Area and Materials

The Western Interior Seaway was a shallow inland sea that extended from the Arctic Ocean to the Gulf of Mexico during the latter half of the Cretaceous (113 mya – 66 mya). North America was separated into two landmasses: Appalachia in the east and Laramidia in the west. During maximum transgression, the seaway was approximately 970 km wide and 3200 km long, but was probably never more than approximately 200 m deep (Sageman and Arthur, 1994).

Many marine paleoenvironments from the Cretaceous are preserved in the shale and limestone deposits across the Great Plains Region. Ammonites from Western Interior Seaway shales were included in this study due to the large number of specimens and the high quality of suture preservation present in these stratigraphic formations. Formations studied include the Mowry Shale, Graneros Shale, Greenhorn Shale, Carlile Shale, and Pierre Shale. This study was limited to organisms with ammonitic sutures, as ammonoids with goniatic and ceratitic sutures were not present in the time periods examined. Ammonoids with straight (n = 127), coiled (n = 210), and heteromorphic (n = 51) shell forms were used to examine the relationship between suture pattern and shell form, and suture pattern and stratigraphic formation.

The Graneros Shale Formation was deposited in the middle Albian and Cenomanian Age of the Cretaceous Period (113.0 mya – 93.9 mya). This formation represents the first episode of offshore marine sedimentation in the central part of the

Western Interior Seaway during the early transgression of the Greenhorn Marine Cycle (Kauffman, 1985). It is approximately 10 m thick in Kansas and as thick as 60 m in Colorado. It consists of a bluish-gray, non-calcareous shale with few beds of sandstone and sandy shale (Fox, 1962; Figure 3). The ammonite specimens from the Graneros Shale included in this study are from Colorado (n = 7), Kansas (n = 15), Texas (n = 2), and South Dakota (n = 1), and represent coiled (n = 25) and heteromorphic (n = 1) shell forms (Appendix A).

The Mowry Shale is a geologic formation that was deposited in the Cenomanian Age of the Cretaceous Period (100.5 mya – 93.9 mya). It is approximately 50 m thick and consists of highly siliceous, hard gray shales with numerous interbedded thin bentonite beds (Nixon, 1973). The Mowry Shale Formation is most abundant in Wyoming and Colorado, reaching into the western-most parts of Nebraska and South Dakota (Figure 3). Its stratigraphic position is equivalent to the middle of the Graneros Formation of Kansas and Colorado (Figure 3). The ammonite specimens from the Mowry Shale that were included in this study are from Montana (n = 7), Texas (n = 12), and Wyoming (n = 10), and represent coiled (n = 28) and straight (n = 1) shell forms (Appendix B).

The Greenhorn Formation consists of four alternating members of shale and limestone. Only ammonite specimens from the shale members – the Hartland and Pfeifer Shales – were included in this study. The Greenhorn Formation can be found in eastern Colorado and Wyoming, northeastern New Mexico, southwestern Montana, and extending east as far as Kansas, Nebraska, and South Dakota (Wilmarth, 1935).

The Hartland Shale Member of the Greenhorn Formation was deposited in the late Cenomanian Age of the Cretaceous Period (100.5 mya – 93.9 mya) as one of the Greenhorn's lower members (Figure 3). It is approximately 25 m thick and consists of calcareous shale with an upper part of thin, chalky limestone beds and a lower part of chalky shale with thin crystalline limestone (Fox, 1962). The ammonite specimens from the Hartland Shale that were included in this study are from Kansas (n = 1), Montana (n = 2), South Dakota (n = 10), and Wyoming (n = 4), and represent coiled (n = 15) and straight (n = 2) shell forms (Appendix C).

The Pfeifer Shale Member of the Greenhorn Formation was deposited in the early Turonian Age of the Cretaceous Period (93.9 mya – 92.3 mya). It is approximately 5 m thick in Kansas and consists primarily of chalky shale (Fox, 1962; Figure 3). The ammonite specimens from the Pfeifer Shale included in this study are from Colorado (n = 1), South Dakota (n = 1), Kansas (n =1), Oklahoma (n = 1), and Wyoming (n = 2), and represent coiled (n = 5) and straight (n = 1) shell forms (Appendix C).

The Carlile Shale was deposited in the middle to late Turonian Age of the Cretaceous Period (93.9 mya – 90.5 mya).  It is approximately 90 m thick and consists of non-calcareous shale to less sandy, very calcareous shale (Fox, 1962; Figure 3).  This Formation is found in western Kansas, southeastern Colorado, and New Mexico. The ammonite specimens from the Carlile Shale included in this study are from Colorado (n = 2), Kansas (n = 35), Montana (n = 8), New Mexico (n = 2), South Dakota (n = 26), Texas (n = 1), and Wyoming (n = 11), and represent coiled (n = 37), straight (n = 23), and heteromorphic (n = 24) shell forms (Appendix D).

The Pierre Shale Formation was deposited during the Campanian Age of the Cretaceous Period (83.6 mya – 72.1 mya). It is approximately 210 m thick at the type locality and overlies the Niobrara Formation (Bertog, 2010; Figure 3). It consists of dark-gray fossiliferous shale with gypsum veins and iron oxide concretions. Its dark color indicates a high organic carbon content, implying a low oxygen environment during deposition and lack of decay on the ocean floor. The Pierre Shale was deposited when the Great Plains were under the deepest portion of the Western Interior Seaway (Schultz et al., 1980). The ammonite specimens from the Pierre Shale included in this study are from Colorado (n = 70), Kansas (n = 23), Montana (n = 24), New Mexico (n = 2), South Dakota (n = 72), Utah (n = 2), and Wyoming (n = 65), and represent coiled (n = 110), straight (n = 122), and heteromorphic (n = 26) shell forms (Appendix E).

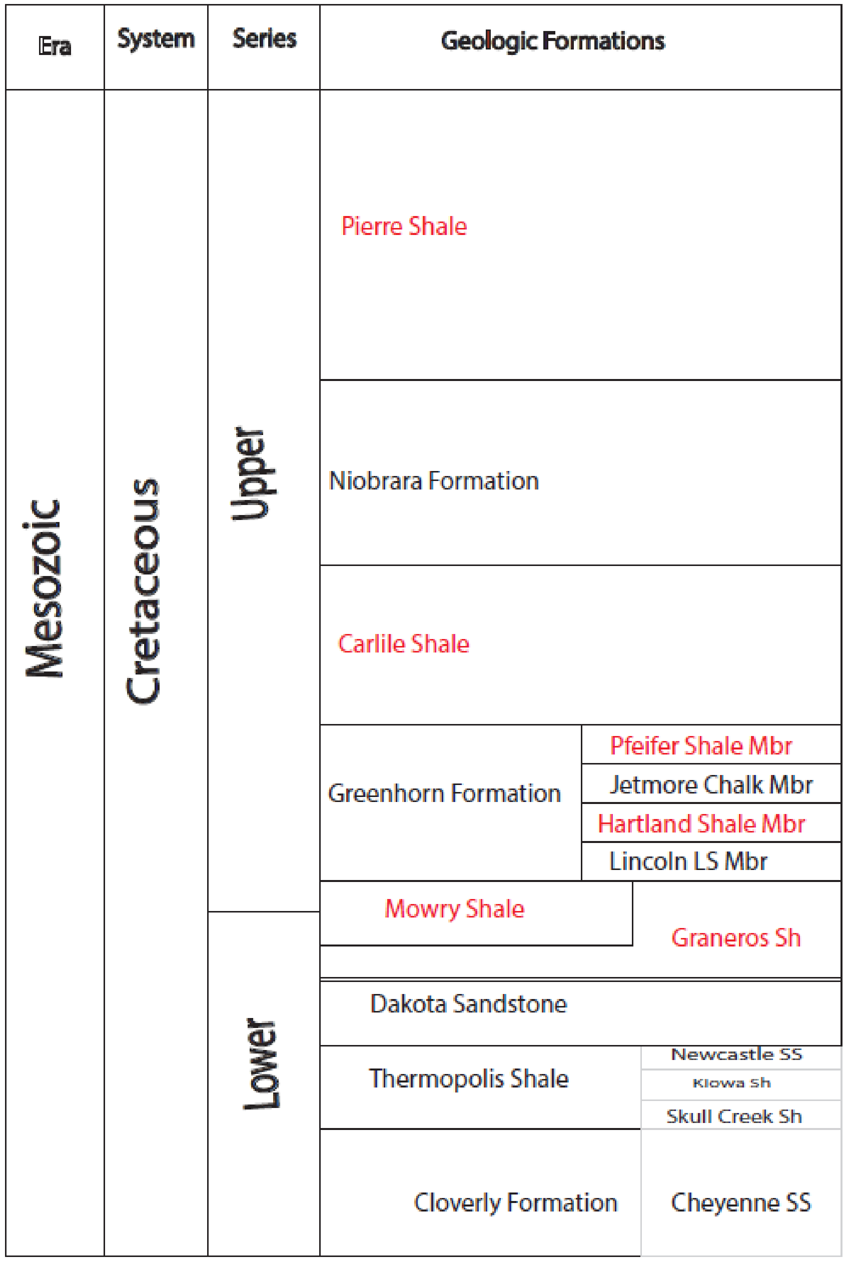


Figure 3: **Western Interior Seaway Stratigraphic Column:** Stratigraphic column of the Western Interior Seaway ranging north to South Dakota, south to Texas, west to Wyoming and east to Kansas. The light lines (bottom right) show stratigraphic formations that are coeval but from different geographic regions. The red text indicates the formations sampled for this study.

Because ammonite suture patterns change through ontogeny, only mature specimens were used for this analysis. Signs of maturity are (1) slowed growth, showing crowded and overlapping sutures; (2) weakening or disappearance of the sculptural elements in the body chamber; (3) modification of the ornamentation near the peristome; (4) modification of the body chamber through a change in coiling; and (5) development of lappets and rostra in the peristome (Sarti, 1999). Of these, septal crowding is the most widely recognized and cited indication of maturity in ammonoids (Kennedy and Cobban, 1976; Gygi, 1990; Gygi, 1999; Sarti, 1999; Gygi, 2001; Monks and Palmer, 2002; Klug et al., 2015). Septal crowding affects the distance of at least the last two septa and occurs when the distance (typically measured by angles) between septa has decreased (Klug et al., 2015). Mature specimens were chosen based on this decreased distance between septa.

## Defining Suture Complexity

Specimens were photographed using a Canon PowerShot 180, 20-megapixel camera. The specimens were photographed at macro level to ensure the suture patterns would be visible. Extraneous features – such as nacre, ribbing, and ornamentation – were removed using the ImageJ photo manipulation software, as these features can cause the analysis to shift focus away from the suture patterns.

A photograph of each specimen was analyzed to determine suture complexity using the FracLac fractal analysis extension for ImageJ. As sutures typically appear as a different color than the shell, FracLac automatically converts the image to binary, which allows the computer to look at the difference in color as data. FracLac defaults for grid design and scaling method were used. The suture complexity of each specimen was quantified using Box-Counting Fractal Analysis ($D_b$). The program samples the image several times using Koch's Curve to increase the number of grid cells, and the results from these samplings are averaged providing the fractal dimension for the specimen. The fractal dimension – a ratio providing a statistical index of complexity comparing how details in a pattern change with scale – is calculated using $D_b = \frac{\log(N_a) - \log(b)}{\log\left(\frac{1}{s_a}\right) - \log\left(\frac{1}{s_b}\right)}$, where N is the number of grid cells in which the suture pattern is present and 1/s is the grid cell size (Kennedy and Cobban, 1976; Figure 4). This fractal dimension is the quantified suture complexity.

Statistical Analysis

Data were separated into three categories within each stratigraphic formation based on shell form: coiled, straight, and heteromorphic. Although coiled and heteromorphic forms were represented by multiple taxa, the straight-shelled forms analyzed where predominately *Baculites.* While *Baculites* are phylogenetically heteromorphs, they are considered a straight-shell form for this analysis because they are the only heteromorph that have completely uncoiled and reverted to the basal straight form.

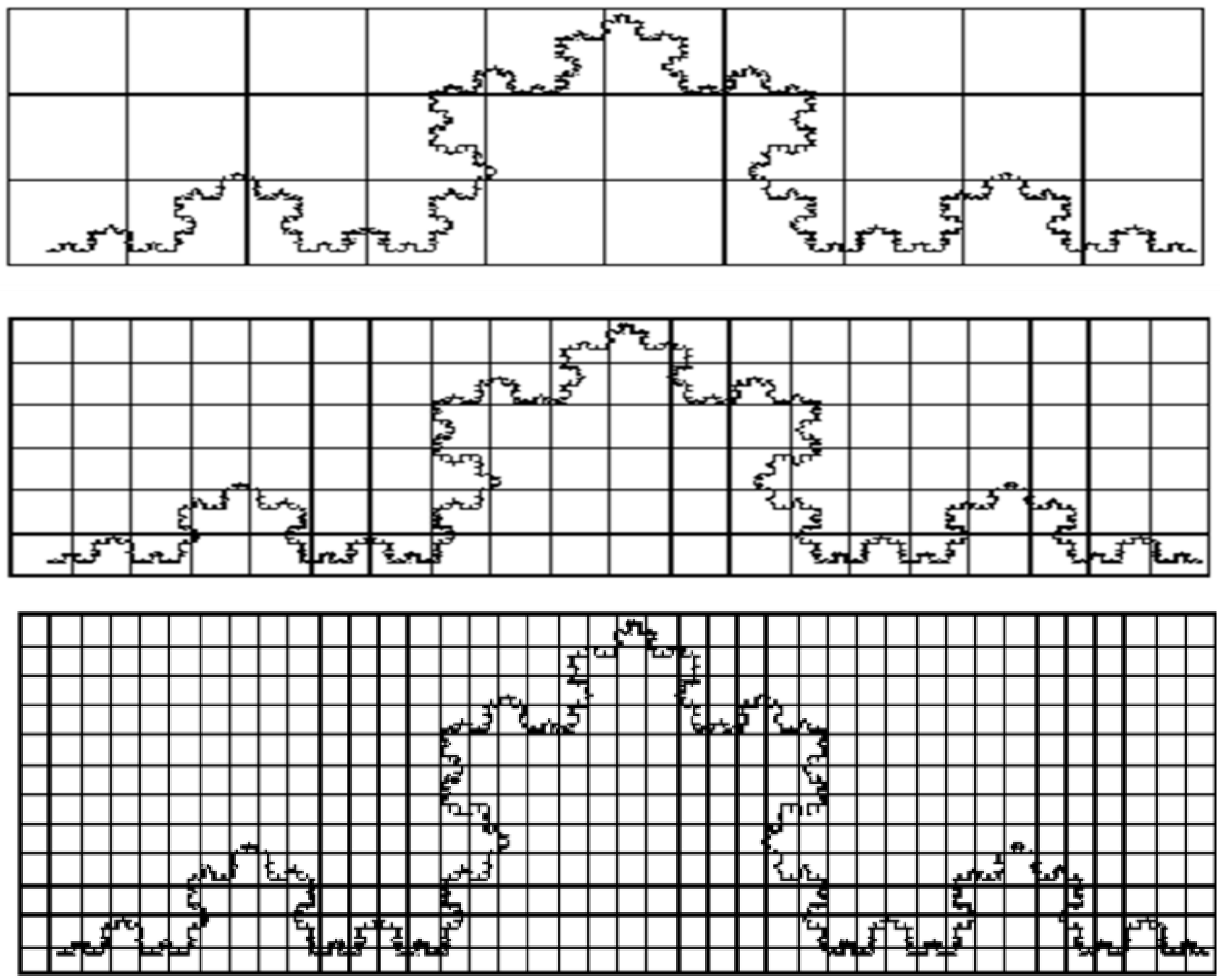

Figure 4: **Box-Counting of Fractal Pattern using Koch's Curve**: The counts where the fractal appears (N) in these images are 18, 41, and 105 grid cells respectively. The three grid size ratios were 1: ½: ¼. The complexity of a fractal is quantified by $D_b = \frac{\log(N_a) - \log(b)}{\log\left(\frac{1}{S_a}\right) - \log\left(\frac{1}{S_b}\right)}$. After placing the counts and ratios into the equation and averaging the three results, the fractal dimension for the above image was found to be 1.27 ± 0.002. Figure from Wahl (1994).

Specimens from each stratigraphic formation were also separated into Mowry, Graneros, Greenhorn, Carlile, and Pierre shales regardless of shell form. The Hartland and Pfeifer Members of the Greenhorn Formation were combined due to small sample size. To eliminate confounding variables, shell forms that were significantly different from each other were removed from the stratigraphic formation analysis.

A Kruskal-Wallis test was used to determine if there were significant differences in median suture complexities among the three shell forms or among the stratigraphic formations (Glantz, 2005). The Kruskal-Wallis test can only indicate if a significant difference exists, but not among which categories. Therefore, if a significant result was indicated by the Kruskal-Wallis test, a Kruskal-Wallis multiple comparison test was used to further delineate differences. The non-parametric Kruskal-Wallis test was chosen over the parametric analysis of variance (ANOVA) because the fractal dimension data did not meet assumptions required for the ANOVA and data transformations were not able to correct for non-normality.

Before performing Kruskal-Wallis tests, the data had to be subset to ensure relatively equal sample sizes from each shell form and each stratigraphic formation. When multiple statistical tests are performed, the Type I statistical error rate (the rate at which the test falsely rejects a null hypothesis) increases. This inflation in the Type I error rate – the Bonferroni Inequality – can be corrected by lowering the significance level of each test. Therefore, the significance level for the Kruskal-Wallis tests performed for this study was lowered ($\alpha = 0.03$) using a Bonferroni correction. All statistical tests were completed using the statistical program R (ver. 3.2.3).

# RESULTS

Results from the Kruskal-Wallis statistical test indicate there is a significant difference in median suture complexity among the shell forms ($H = 27.9$, $df = 2$, $p < 0.001$). A Kruskal-Wallis multiple comparisons test indicates that median coiled shell sutures are significantly more complex than median heteromorphic shell sutures ($p < 0.03$). Median straight shell sutures are more complex than median heteromorphic shell sutures ($p < 0.03$). However, there is no significant difference in median suture complexity between straight and coiled shell forms ($p > 0.03$; Figure 5, Table 1).

Table 1: **Median Suture Complexity of Shell Forms for Ammonite Specimens**

| | Coiled | Straight | Heteromorph |
|---|---|---|---|
| Complexity | 1.762 | 1.755 | 1.719 |

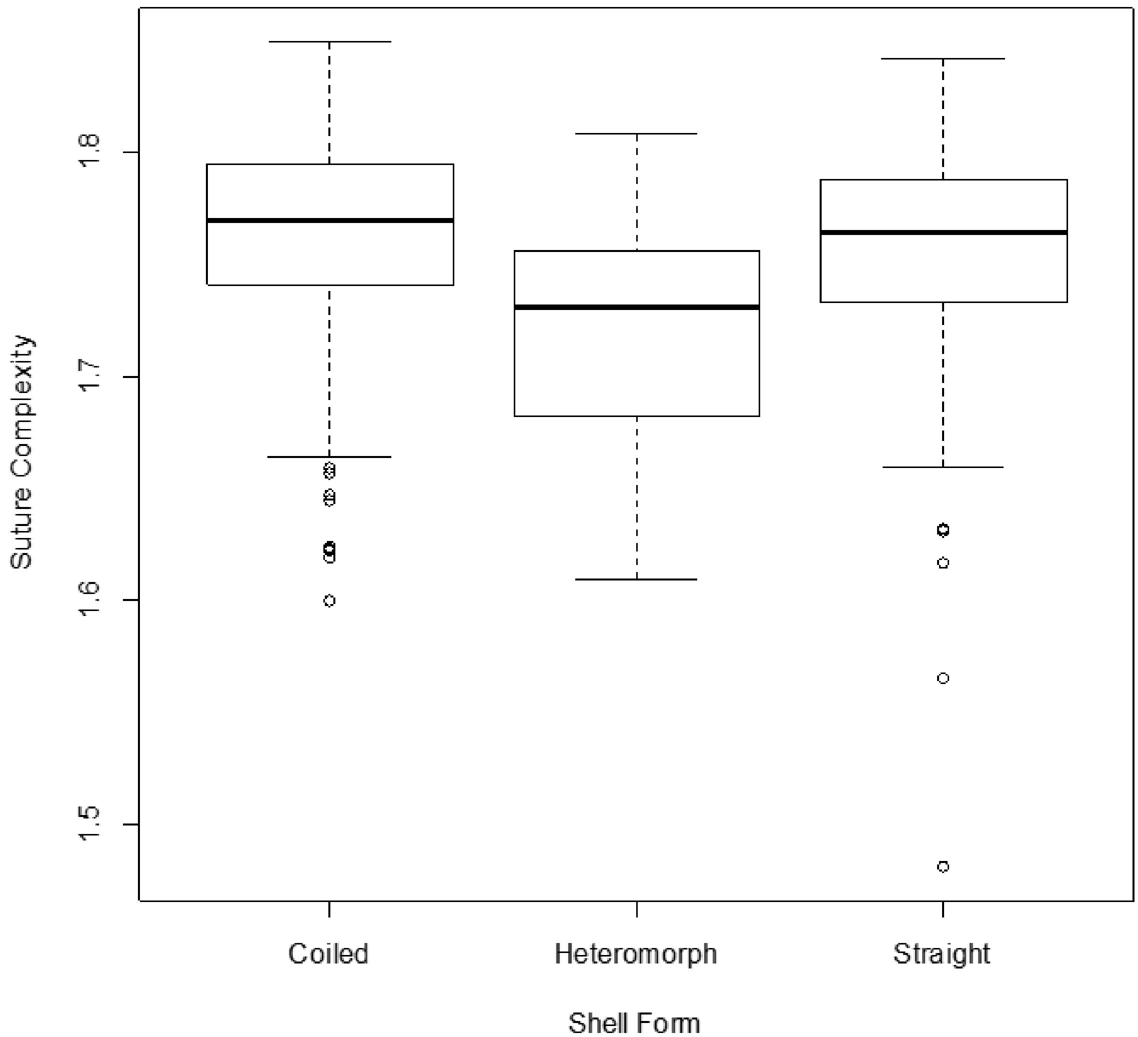


Figure 5: **Suture Complexity of Ammonite Shell Forms from the Western Interior Seaway**: In this figure, the solid, black bars indicate the median suture complexity for each shell form.

A Kruskal-Wallis statistical test was also completed to determine if there was a significant difference among median suture complexities of ammonite specimens from the Mowry Shale (n = 28), Graneros Shale (n = 23), Greenhorn Shale members (n = 20), Carlile Shale (n = 34), and Pierre Shale (n = 35). Results indicate there is no significant difference in median suture complexity among stratigraphic formations (H = 5.24, df = 4, p = 0.264; Figure 6, Table 2).

Table 2: **Median Suture Complexity of Ammonite Specimens from Shale Formations**

| | Mowry | Graneros | Greenhorn | Carlile | Pierre |
|---|---|---|---|---|---|
| Complexity | 1.752 | 1.741 | 1.755 | 1.736 | 1.760 |

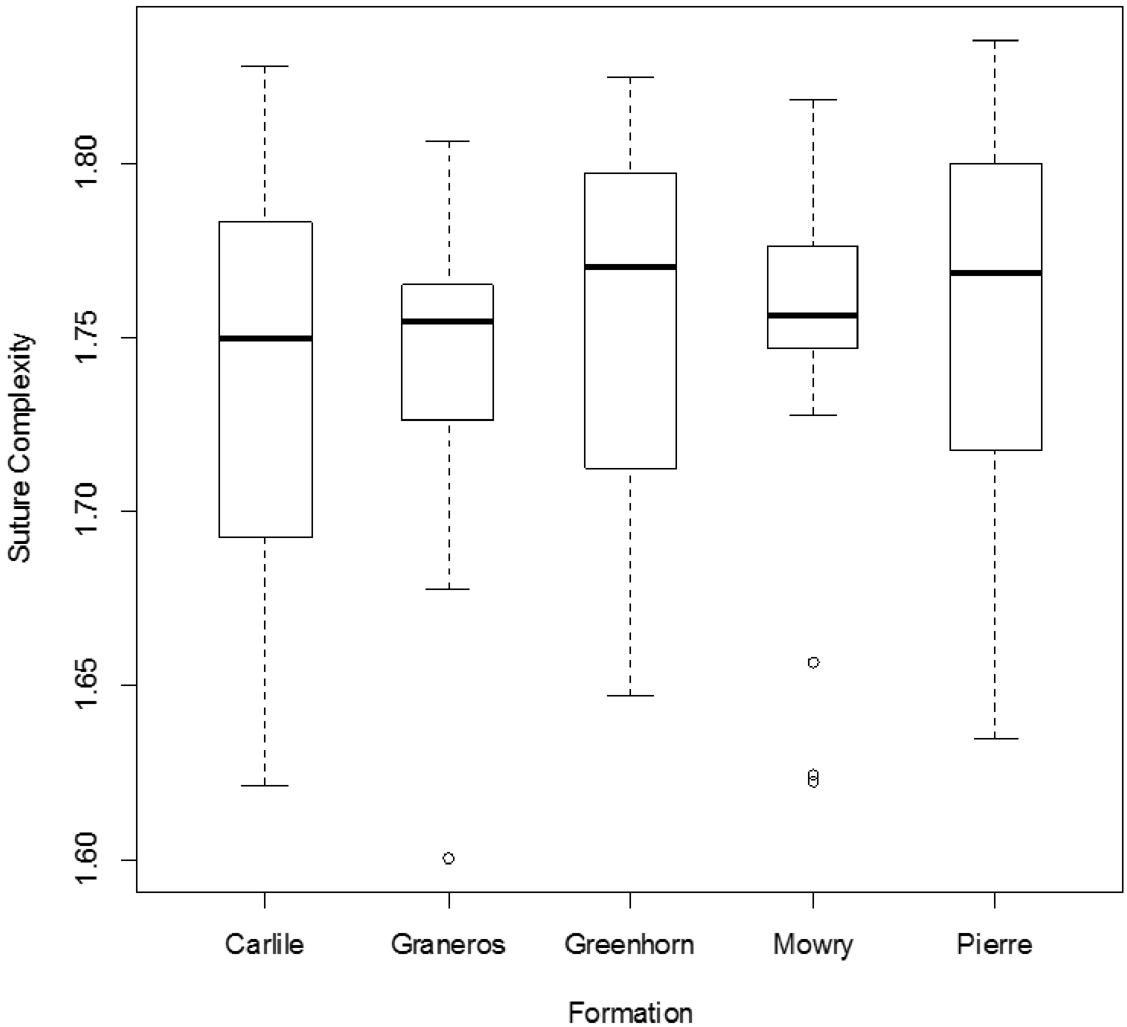


Figure 6: **Suture Complexity of Ammonites from Western Interior Seaway Shales**: In this figure, the solid, black bars indicate the median suture complexity for each formation.

# DISCUSSION

While ammonite suture patterns have been studied for many decades, suture complexity has not been compared among shell forms. The results of this study indicate that there are significant differences in suture pattern complexity among the shell forms, and that complex suture patterns might may have aided the coiling process and provided increased protection against hydrostatic pressure.

Coiled shells were found to have the most complex suture patterns of the three shell forms examined (though not significantly different from straight shells). This lends support to the hypothesis that complex suture patterns evolved to support the shell as it coiled (Jacobs, 1990). A complex suture pattern would allow more surface area for septa attachment between the septal joints, providing interlocking strength and allowing a tighter coil (Drew and Pelligrino, 2002; Miura et al., 2009).

Heteromorphic and secondarily straight forms, such as *Baculites*, evolved from the coiled shell form, uncoiling their shells over evolutionary time (Mikhailova and Baraboshkin, 2009). Like coiled forms, heteromorphic forms still had a partially rounded shell to distribute the force of hydrostatic pressure (Lu et al., 1998). Results from this study find heteromorphic and *Baculites* shells to have less complex suture patterns than their coiled relatives. Assuming complex sutures are necessary to aid tight coiling (as hypothesized above), heteromorphic ammonites would not have needed to retain highly complex sutures. This could explain the reduction in suture complexity of heteromorphic forms as lineages underwent the uncoiling process through their evolutionary history. It is unknown why heteromorphic ammonites uncoiled their shells or whether suture patterns became less complex before the shell started this uncoiling process, but those questions are outside the focus of this project.

Unexpectedly, *Baculites* had more complex sutures than heteromorphic forms, though not significantly different from coiled forms. This indicates that *Baculites* retained complexity similar to their coiled ancestors. A straight shell is not able to spread force as effectively as coiled forms, and is, therefore, more susceptible to damage from hydrostatic pressure (Li et al., 2011). Complex suture patterns that were important to the coiling process in coiled forms might have been exapted to protect the straight shell against hydrostatic pressure, acting in a similar manner to corrugated metal (Boletzky, 1999). This exaptation could explain why suture complexity is not significantly different between coiled and straight-shelled forms.

Additionally, it has been suggested that suture patterns of *Baculites* were adapted to form ribbing that further protected the organism from hydrostatic pressure (Jacobs, 1990). The ribbing might have acted as a keel, pressing out as pressure pushed in on the shell. Susceptibility to hydrostatic pressure could also explain why there are relatively few genera in the Baculitidae clade compared to the diverse clades found among the coiled shell forms such as Collignoniceratidae. The straight-shelled forms were not as successful as the coiled and, therefore, did not diversify like their coiled counterparts.

Ammonites are hypothesized to have hunted at the lower edge of the photic zone (Pasche and May, 2001). Some ammonites are thought to have fed at great depths with a wide range of vertical mobility, but most were probably vertical migrants in the mesopelagic zone, like extant nautiloids (Westermann, 1996). For each 10 m of water below the surface, the water pressure increases by approximately 0.987 atm (Saunders, 1981). Therefore, organisms must adjust to changing pressures as they move vertically in the water column. If ammonites were vertical migrants, they might have evolved more complex shell sutures, compared to earlier ceratitic and goniatic clades, to protect their shell from intense changes in hydrostatic pressure.

Attributing depths in the water column for ammonites has proven difficult due to the large range of habitats utilized by their closest living relatives (Nesis, 1987). It has been hypothesized that different ammonite forms had different niches, which led to the development of the three forms (Jacobs, 1990). The straight-shelled forms perhaps lived in the middle of the water column or near shoals (Westermann, 1996), heteromorphic ammonites perhaps lived in shallower waters at depths of 30-100 m (Pasche and May, 2001), and the coiled shell forms might have lived in deeper environments, like nautiloids today (Nesis, 1987). If the different forms of ammonites had different niches, the suture patterns might have evolved to an optimal complexity for the shell form's particular niche. However, more research will need to be completed to support or reject these hypotheses.

This study also analyzed whether there is a relationship between ammonite suture complexity and stratigraphic formation from the Western Interior Seaway. The lack of a significant difference in suture complexity among formations could be explained by the shales included in this study representing similar depositional conditions. These similar conditions could contribute to differences in suture complexity among the stratigraphic formations being difficult to detect (Table 2). Western Interior Seaway shales were probably deposited in stratified, deep, still water off-shore from beach sands (Chamley, 1991). The black color of these shales implies that they formed in oxygen-deficient environments at the water-sediment interface. If more oxygen had been present, the organic matter would have fully decayed, not leaving the dark coloring. This oxygen-poor environment also allowed for sulfide minerals such as pyrite to form, which covered portions of the preserved specimens (Holland, 1979).

Even if organisms lived in a range of environments above the depositional zone, organisms from all environments in the water column would have fossilized within the same depositional zone. Therefore, each formation represents a mixing of environments that existed in the water column above its depositional zone. This mixing could lead to an averaging that could result in the lack of significant differences found among ammonites from different formations.

# CONCLUSION

Ammonites of the Western Interior Seaway exhibit significantly different shell suture complexities among coiled, heteromorphic, and straight forms. The most complex suture patterns were found in tightly-coiled shells, possibly adding structural support to the coil. Heteromorphic shell forms have significantly less complex sutures than those of straight and coiled shell forms. Heteromorphic shell forms might have significantly reduced their suture complexity to loosen the coil of their shell. These forms might not have required suture patterns as complex as the straight shell forms because their partially coiled shells would have provided similar protection against hydrostatic pressure to the coiled form. Most of the straight-shelled forms examined in this study evolved from coiled forms and might have exapted highly complex sutures to protect against hydrostatic pressure. This could explain why they have more complex sutures than heteromorphic forms.

Ammonite suture complexity did not show a significant difference among stratigraphic formations. The formations studied represent similar depositional conditions, which could potentially explain this lack of significant difference.

Future work will include studying a wider range of stratigraphic formations and comparing goniatic and ceratitic suture patterns to ammonitic suture patterns to determine if there is a progression of complexity among differing shell forms. Other goals of future research are to distinguish niche partitioning in the ammonitic shell forms and examine taxonomic bias of suture preservation.

# REFERENCES CITED


Allen, E.G. 2006. New approaches to Fourier analysis of ammonoid sutures and other complex, open curves. Paleobiology 32:299–315.

Allen, J.B. 1977. Short Time Spectral Analysis and Modification by Discrete Fourier Transformation. IEEE Transactions on Acoustics, Speech, and Signal Processing 25: 235-238.

Bertog, J. 2010. Stratigraphy of the Lower Pierre Shale (Campanian): Implications for the Tectonic and Eustatic Controls on Facies Distributions. Journal of Geological Research 2010:1-15.

Boletzky, S. 1999. Cephalopod development and evolution: biological insight into ontogenesis as a guide to paleomorphology. Advancing Research on Living and Fossil Cephalopods 124:271–278.

Boyajian, G. and T. Lutz. 1992. Evolution of biological complexity and its relation to taxonomic longevity in the Ammonoidea. Geology 20:983.

Chamley, H. 1991. Environment of Epicontinental Seas. Gauthier-Villars, Montrouge, pp. 111-188.

Daniel, T.L., B.S. Helmuth, W.B. Saunders, and P.D. Ward. 1997. Septal complexity in ammonoid cephalopods increased mechanical risk and limited depth. Paleobiology 23:470-481.

Drew, H.R. and S. Pellegrino. 2002. New Approaches to Structural Mechanics, Shells, and Biological Structures. Springer, Cambridge, pp. 216-220.

Dzik, J. 1984. Phylogeny of the Nautiloidea. Palaeontologia Polonica 45:1-219.

Fox, C. S. 1962. Stratigraphy. Kansas Geological Survey 156.

Glantz, S. A. 2005. Primer of Biostatistics. McGraw-Hill Medical Pub., New York, pp. 20.

Gygi, R.A. 1990a. The Oxfordian ammonite succession near Liesberg BE and Péry BE, northern Switzerland. Ecolgae geologicae Helvetiae 83: 177-199.

Gygi, R.A. 1999. Ammonite ecology in Late Jurassic time in northern Switzerland. Ecologae geologicae Helvetiae 92: 129-137

Gygi, R.A. 2001. Perispinctacean ammonites of the Late Jurassic in norther Switzerland: a versatile tool to investigate the sedimentary geology of an epicontinental sea. Schweizerische Palaontologische Abhandlungen 123:1-232.

Holland, H.D. 1979. Metals in black shales: a reassessment. Economic Geology 70: 1676-1680

Jacobs, D. 1990. Sutural pattern and shell stress in Baculites with implications for other cephalopods shell morphologies. Paleobiology 16:336–348.

Kauffman, E.G. 1985. Depositional History of the Graneos Shale (Cenomanian), Rock Canyon Anticline. Fine-Grained Deposits and Biofacies of the Cretaceous Western Interior Seaway: Evidence of Cyclic Sedimentary Processes FG4: 90-120.

Kennedy, W.J. and W.A. Cobban. 1976. Aspects of Ammonite Biology, Biogeography, and Biostratgraphy. Special Papers in Palaeontology 17: 1-99.

Klug, C. and J. Lehmann. 2015. Soft Part Anatomy of Ammonoids: Reconstructing the Animal Based on Exceptionally Preserved Specimens and Actualistic Comparisons. Topics in Geobiology Ammonoid Paleobiology 515–537.

Klug, C., M. Zatón, H. Parent, B. Hostettler, and A. Tajika. 2015. Mature Modifications and Sexual Dimorphism. Topics in Geobiology: Ammonoid Paleobiology 253-320.

Li, Y., C. Ortiz, and M. C. Boyce. 2011. Stiffness and strength of suture joints in nature. Physical Review E Phys. Rev. E 84.

Lu, M., F-R. Grosche, G.E.A. Meier. 1998. Drag reduction of a sphere at supercritical Reynolds numbers using passive ventilation. IUTAM Symposium on Mechanics of Passive and Active Flow Control 53:127-132.

Lutz, T. and G. Boyajian. 1995. Fractal Geometry of Ammonoid Sutures. Paleobiology 21:329–342.

Manship, L. 2004. Pattern matching; classification of ammonitic sutures using GIS. Palaeontologia Electronica.

Mikhailova, I.A. and E. Yu. Baraboshkin. 2009. The evolution of the heteromorph and monomorph early Cretaceous ammonites of the suborder Ancyloceratina Wiedmann. Paleontological Journal 5:51-60

Miura, T., C.A. Perlyn, M. Kinoboshi, N. Ogihara, M. Kobayashi-Miura, G.M. Morriss-Kay, and K. Shiota. 2009. Mechanism of skull suture maintenance and interdigitation. Journal of Anatomy 215: 642-655.

Monks, N., and P. Palmer. 2002. Ammonites. Smithsonian Institution Press, Washington, D.C., pp.34-50.

Nesis, K.N., 1987. Cephaloods of the World, Squids, Cuttlefish, Octopuses, and Allies. T.F.H. Publications, Neptune City, NJ.

Nixon, R.P., 1973. Oil source beds in Cretaceous Mowry Shale of northwestern interior United States. American Association of Petroleum Geologists Bulletin 57: 136-161.

Olóriz, F., P. Palmqvist, and J. A. Pérez-Claros. 2002. Morphostructural constraints and phylogenetic overprint on sutural frilling in Late Jurassic ammonites. Lethaia 35:158–168.

Pasche, A.D. and K.C. May. 2001. Taphonomy and paleoenvironment of hadrosaur (Dinosauria) from Matanuska Formation (Turonian) in South-Central Alaska. Mesozoic Vertebrate Life 219-236.

Pérez-Claros, J. A., F. Olóriz, and P. Palmqvist. 1997. Sutural complexity in Late Jurassic ammonites and its relationship with phragmocone size and shape: a multidimensional approach using fractal analysis. Lethaia 40:253–272.

Sageman, B.B. and Arthur, M.A. 1994. Early Tuornian Paleogeographic/Paleobathymetric Map. Western Interior. U.S. Mesozoic Systems of the Rocky Mountain Region. pp.457-469

Sarti, C. 1999. Whorl width in the body chamber of ammonites as a sign of dimorphism. Advancing Research on Living and Fossil Cephalopods 315-332.

Saunders, P.M. 1981. Practical conversion of pressure to depth. Journal of Physical Oceanography 11: 573-574.

Schultz, L.G., H.A. Tourtelot, J.R. Gill, and J.G. Boerngen. 1980. Composition and Properties of the Pierre Shale and Equivalent Rocks of Late Cretaceous Age. Geological Survey Professional Paper 1064-B: 9-40, 77-81

Vicsek, T. 1992. Fractal growth phenomena. World Scientific 31: 139-146.

Wahl, B. 1994. Exploring Fractals on the Macintosh. Addison-Wesley Professional, New York, pp. 27-75.

Westermann, G. E. G. 1996. Ammonoid Life and Habitat. Topics in Geobiology Ammonoid Paleobiology 607–707.

Wilmarth, M.G. 1935. Lexicon of geologic names of the United States (including Alaska). U.S. Geological Survey Bulletin 896: 1-2, 2396.

Wippich, M. G. E., and J. Lehmann. 2004. Allocrioceras from the Cenomanian (mid-Cretaceous) of the Lebanon and its bearing on the palaeobiological interpretation of heteromorphic ammonites. Palaeontology 47:1093–1107.

Yacobucci, M., and L. Manship. 2011. Ammonoid septal formation and suture asymmetry explored with a geographic information systems approach. Palaeontologia Electronica 14:17.

# APPENDIX A

## Graneros Shale Complexity Data

| Museum # | Identification | State | County | Member | Shell Form | Complexity |
|---|---|---|---|---|---|---|
| USGS_2288 | *Acanthoceras* | Colorado | Pueblo | | Coiled | 1.7987 |
| UT_10708 | *Scaphites hippocrepis* | Texas | | | Heteromorph | 1.6984 |
| UT_11128 | *Acanthoceras* | Texas | | | Coiled | 1.7857 |
| KUIP_150282 | *Plesioacanthoceras amphibolum* | Colorado | Pubelo | | Coiled | 1.7602 |
| KUIP_282251 | *Acanthoceras amphibolum* | Kansas | Ellsworth | | Coiled | 1.6003 |
| KUIP_286262 | *Acanthoceras amphibolum* | Kansas | Wilson | | Coiled | 1.6847 |
| KUIP_286263 | *Acanthoceras amphibolum* | Kansas | Ellsworth | | Coiled | 1.779 |
| KUIP_286321 | *Acanthoceras amphibolum* | Kansas | Ellsworth | | Coiled | 1.7387 |
| KUIP_286338 | *Acanthoceras amphibolum* | Kansas | Ellsworth | | Coiled | 1.7137 |
| KUIP_286340 | *Acanthoceras amphibolum* | Kansas | Ellsworth | | Coiled | 1.7579 |
| KUIP_287411 | *Acanthoceras amphibolum* | Kansas | Ellsworth | | Coiled | 1.7547 |
| KUIP_287650 | *Acanthoceras amphibolum* | Kansas | Ellsworth | | Coiled | 1.7451 |
| KUIP_288066 | *Acanthoceras amphibolum* | Kansas | Wilson | | Coiled | 1.6777 |
| KUIP_288067 | *Acanthoceras amphibolum* | Kansas | Wilson | | Coiled | 1.7033 |
| KUIP_288085 | *Acanthoceras amphibolum* | Kansas | Wilson | | Coiled | 1.7609 |
| KUIP_288089 | *Acanthoceras amphibolum* | Kansas | Ellsworth | | Coiled | 1.7676 |
| KUIP_288098 | *Acanthoceras amphibolum* | Kansas | Ellsworth | | Coiled | 1.7465 |
| USGS_D4428 | *Plesioacanthoceras* | Colorado | Pueblo | | Coiled | 1.7642 |
| USGS_D5126 | *Plesioacanthoceras amphibilum* | Colorado | Pueblo | | Coiled | 1.6909 |
| USGS_D5708 | *Acanthoceras* | Colorado | Pueblo | | Coiled | 1.8069 |
| USGS_D5711 | *Acanthoceras* | Colorado | Pueblo | | Coiled | 1.7493 |
| USGS_D5718 | *Acanthoceras* | Colorado | Pueblo | | Coiled | 1.7794 |
| USGS_D6587 | *Acanthoceras muldoonese* | Colorado | Pueblo | | Coiled | 1.7663 |
| USGS_D7367 | *Acanthoceras* | South Dakota | Fall River | Thatcher | Coiled | 1.7387 |

APPENDIX B

Mowry Shale Complexity Data

| Museum # | Identification | State | County | Shell Form | Complexity |
|---|---|---|---|---|---|
| USGS_224 | *Metengonoceras* | Texas | | Coiled | 1.7543 |
| USGS_339 | *Neogastropolites* | Wyoming | Big Horn | Coiled | 1.7503 |
| FHSMIP_664 | *Metengonoceras* | Montana | | Coiled | 1.7899 |
| USGS_2169 | *Epengonoceras dumbli* | Texas | Grayson | Coiled | 1.7755 |
| USGS_2170 | *Metengonoceras* | Texas | | Coiled | 1.7413 |
| USGS_2176 | *Metengonoceras* | Texas | | Coiled | 1.7497 |
| USGS_2177 | *Metengonoceras* | Texas | | Coiled | 1.7279 |
| USGS_4140 | *Metengonoceras* | Texas | | Coiled | 1.7759 |
| USGS_7320 | *Metengonoceras* | Texas | | Coiled | 1.7595 |
| USGS_9933 | *Metengonoceras dumbli* | Texas | Grayson | Coiled | 1.7507 |
| UT_10423 | *Baculites* | Texas | Travis | Straight | 1.7445 |
| USGS_22614 | *Metengonoceras* | Texas | | Coiled | 1.6244 |
| USGS_23042 | *Metengonoceras* | Wyoming | Wheatland | Coiled | 1.7562 |
| USGS_24065-1 | *Metengonoceras* | Montana | Petroleum | Coiled | 1.7441 |
| USGS_24065-2 | *Neogastropolites muelleri* | Montana | Petroleum | Coiled | 1.757 |
| USGS_24065-3 | *Neogastropolites muelleri* | Montana | Petroleum | Coiled | 1.7894 |
| USGS_24417 | *Metengonoceras* | Texas | | Coiled | 1.7715 |
| USGS_24555 | *Metengonoceras* | Wyoming | Park | Coiled | 1.7832 |
| USGS_24565 | *Metengonoceras* | Wyoming | Park | Coiled | 1.7953 |
| USGS_24567 | *Metengonoceras* | Wyoming | Park | Coiled | 1.8186 |
| USGS_24568 | *Metengonoceras* | Wyoming | Park | Coiled | 1.7764 |
| USGS_26589 | *Ergonoceras* | Montana | Judith Basin | Coiled | 1.7498 |
| UCM_29766 | *Metengonoceras* | Wyoming | Big Horn | Coiled | 1.7748 |
| UT_30675 | *Gastropolites* | Montana | | Coiled | 1.7391 |
| YPMIP_527510 | *Neogastropolites* | Montana | Carbon | Coiled | 1.6567 |
| USGS_D13229 | *Metengonoceras* | Wyoming | Big Horn | Coiled | 1.6226 |
| USGS_D1738 | *Neogastropolites* | Wyoming | Hot Springs | Coiled | 1.7765 |
| USGS_D9496 | *Epengonoceras* | Texas | Fannin | Coiled | 1.7522 |

# APPENDIX C

## Greenhorn Complexity Data

| Museum # | Identification | State | County | Member | Shell Form | Complexity |
|---|---|---|---|---|---|---|
| FHSMIP_531 | *Baculites* | Kansas | Smith | Hartland | Straight | 1.7955 |
| UT_4269 | Ammonitida | Oklahoma | Cimarron | Pfeifer | Coiled | 1.7157 |
| USGS_12610 | *Thomasites* | Colorado | Larimer | Pfeifer | Coiled | 1.7298 |
| USGS_12658 | *Metoriceras* | Wyoming | | Pfeifer | Coiled | 1.7951 |
| USGS_22817 | *Proplacenticeras pseudoplacenta* | Wyoming | Natrona | Hartland | Coiled | 1.81 |
| USGS_22871 | *Acanthoceras wyomingensis* | Montana | | Hartland | Coiled | 1.7981 |
| USGS_23153 | *Pachydiscus* | Wyoming | Natrona | Hartland | Coiled | 1.8253 |
| SDSM_43554 | *Metoicoceras gilinanum* | South Dakota | | Hartland | Coiled | 1.7768 |
| SDSM_112541 | Ammonitida | South Dakota | | Hartland | Coiled | 1.796 |
| YPMIP_850126 | Ammonitida | South Dakota | Butte | Hartland | Coiled | 1.7971 |
| YPMIP_850127 | Ammonitida | South Dakota | Butte | Hartland | Coiled | 1.8061 |
| YPMIP_850128 | Ammonitida | South Dakota | Butte | Hartland | Coiled | 1.7091 |
| YPMIP_850129 | Ammonitida | South Dakota | Butte | Hartland | Coiled | 1.7414 |
| YPMIP_850132 | Ammonitida | South Dakota | Butte | Hartland | Coiled | 1.647 |
| YPMIP_850133 | Metoicoceras | South Dakota | Butte | Hartland | Coiled | 1.6645 |
| USGS_33-8 | *Acanthoeras wyomingensis* | Montana | | Hartland | Coiled | 1.8021 |
| USGS_D10512 | *Calycoceras obrieni* | South Dakota | Lawrence | Hartland | Coiled | 1.6906 |
| USGS_D11560 | *Dunveganoceras* | Wyoming | Weston | Pfeifer | Coiled | 1.7637 |
| USGS_D12917 | *Proplacenticeras* | South Dakota | Pennington | Pfeifer | Coiled | 1.7444 |
| USGS_D13182 | *Calycoceras* | South Dakota | Butte | Hartland | Coiled | 1.7839 |
| USGS_D624 | *Baculites* | Kansas | | Pfeifer | Straight | 1.7822 |
| USGS_D783 | *Baculites* | Wyoming | Natrona | Hartland | Straight | 1.7829 |
| USGS_D9805 | *Borrisiakoceras* | Wyoming | | Hartland | Coiled | 1.7055 |

APPENDIX D

Carlile Shale Complexity Data

| **Museum #** | **Identification** | **State** | **County** | **Member** | **Shell Form** | **Complexity** |
|---|---|---|---|---|---|---|
| FHSMIP_666 | *Baculites* | Kansas | Smith | | Straight | 1.8043 |
| FHSMIP_832 | Ammonitida | Kansas | Osborne | Blue Hill | Coiled | 1.7881 |
| FHSMIP_901 | *Proplacenticeras pseudoplacenta* | Kansas | Trego | Blue Hill | Coiled | 1.8188 |
| UT_968 | *Baculites* | Montana | Hot Springs | | Straight | 1.6847 |
| UT_970 | *Baculites* | Montana | Hot Springs | | Straight | 1.6926 |
| UT_978 | *Baculites* | Montana | Hot Springs | | Straight | 1.7808 |
| USGS_1202 | *Baculites* | Kansas | Logan | | Straight | 1.7657 |
| USGS_1396 | *Baculites* | Kansas | Logan | | Straight | 1.7959 |
| USGS_1411 | *Baculites* | Kansas | Logan | | Straight | 1.6312 |
| USGS_1477 | *Baculites* | Kansas | Logan | | Straight | 1.704 |
| SDSM_1507 | *Prionocyclus wyomingensis* | South Dakota | Fall River | | Coiled | 1.7654 |
| USGS_1571 | *Baculites* | Kansas | Logan | | Straight | 1.8051 |
| UT_1635 | *Baculites* | New Mexico | Union | | Straight | 1.6317 |
| UT_1672 | *Priontropis woolgari* | South Dakota | Fall River | | Coiled | 1.6698 |
| USGS_2967-1 | *Prionocyclus wyomingensis* | South Dakota | Meade | | Coiled | 1.7649 |
| USGS_2967-2 | *Baculites* | South Dakota | Meade | | Straight | 1.7251 |
| DMNS_4049 | *Prionocyclus macombi* | South Dakota | Fall River | | Coiled | 1.7964 |
| DMNS_4129 | *Baculites yokoyami* | South Dakota | Butte | | Straight | 1.7086 |
| DMNS_4157 | *Scaphites whitfieldi* | South Dakota | Fall River | | Heteromorph | 1.6096 |
| DMNS_7856 | *Baculites crickmayi* | South Dakota | Fall River | | Straight | 1.8038 |
| UT_10571 | *Desmoscaphites* | Montana | Big Horn | | Heteromorph | 1.7991 |
| UT_10703 | *Desmoscaphites* | Montana | Big Horn | | Heteromorph | 1.6945 |
| UT_11129 | *Scaphites venericosus depressus* | Montana | Big Horn | | Heteromorph | 1.795 |
| USGS_12642 | *Puzosia* | South Dakota | | | Coiled | 1.7841 |
| USGS_14696 | Ammonitida | Kansas | Osborne | Blue Hill | Coiled | 1.7203 |
| UCM_18386 | *Prioncyclus hyatti* | Kansas | Osborne | | Coiled | 1.7505 |
| USGS_21187 | *Prionocyclus* | South Dakota | Butte | | Coiled | 1.7922 |
| USGS_21192-1 | *Prionocyclus* | South Dakota | Butte | | Coiled | 1.6239 |

| | | | | | | |
|---|---|---|---|---|---|---|
| USGS_21192-2 | *Prionocyclus* | South Dakota | Butte | | Coiled | 1.7851 |
| USGS_21194-1 | *Prionocyclus* | South Dakota | Butte | | Coiled | 1.7 |
| USGS_21194-2 | *Prionocyclus wyomingensis* | South Dakota | Butte | | Coiled | 1.768 |
| USGS_21197 | *Prionocyclus* | South Dakota | Butte | | Coiled | 1.7343 |
| USGS_21199 | *Prionocyclus* | South Dakota | Butte | | Coiled | 1.7704 |
| USGS_21424 | Ammonitida | Wyoming | Crook | | Coiled | 1.7287 |
| USGS_21838 | *Prionocyclus hyatti* | South Dakota | Meade | | Coiled | 1.7557 |
| USGS_21838 | *Scaphites aracdiensis* | Wyoming | | | Heteromorph | 1.7581 |
| USGS_22871 | Ammonitida | South Dakota | Fall River | | Coiled | 1.7807 |
| USGS_23474 | *Prionocyclus* | South Dakota | Butte | | Coiled | 1.7635 |
| KUIP_32027 | *Scaphites calilensis* | Kansas | Mitchell | | Heteromorph | 1.7751 |
| KUIP_32031 | *Scaphites pygaeus* | Kansas | Mitchell | Blue Hill | Heteromorph | 1.6873 |
| KUIP_32033 | *Scaphites pygmaeus* | Kansas | Mitchell | Blue Hill | Heteromorph | 1.6397 |
| UT_36374 | *Prionocyclus hyatti* | Kansas | Ellis | Blue Hill | Coiled | 1.7821 |
| UT_36375 | *Prionocyclus novimexicanus* | South Dakota | Fall River | | Coiled | 1.7893 |
| UT_36383 | *Prionocyclus novimexicanus* | South Dakota | Fall River | | Coiled | 1.767 |
| UT_36865 | *Baculites* | Colorado | Pitkin | | Straight | 1.7141 |
| UT_38294 | *Baculites* | Montana | Hot Springs | | Straight | 1.7644 |
| UT_41543 | Ammonitida | Colorado | Montezuma | | Coiled | 1.7912 |
| KUIP_58911 | *Proplacenticeras pseudoplacenta* | Kansas | Bloomington | Blue Hill | Coiled | 1.7931 |
| KUIP_58912 | *Proplacenticeras pseudoplacenta* | Kansas | Ellis | Blue Hill | Coiled | 1.7794 |
| UT_63025 | *Prionocyclus novimexicanus* | Wyoming | Big Horn | | Coiled | 1.7534 |
| KUIP_65849 | *Prionocyclus hyatti* | Kansas | Mitchell | Blue Hill | Coiled | 1.7076 |
| KUIP_108769 | *Scaphites arcadiensis* | Kansas | Mitchell | Blue Hill | Heteromorph | 1.6667 |
| KUIP_108770 | *Scaphites kansiensis* | Kansas | Mitchell | Blue Hill | Heteromorph | 1.7262 |
| KUIP_108774 | *Scaphites calilensis* | Kansas | Mitchell | Blue Hill | Heteromorph | 1.6716 |
| KUIP_108776 | *Scaphites calilensis* | Kansas | Mitchell | Blue Hill | Heteromorph | 1.7504 |
| KUIP_108778 | *Scaphites calilensis* | Kansas | Mitchell | Blue Hill | Heteromorph | 1.7466 |
| KUIP_108780 | *Scaphites carlilensis* | Kansas | Mitchell | Blue Hill | Heteromorph | 1.6754 |
| KUIP_108806 | *Scaphites inflexus* | Kansas | Mitchell | Blue Hill | Heteromorph | 1.7305 |
| KUIP_108807 | *Scaphites hattini* | Kansas | Mitchell | Blue Hill | Heteromorph | 1.7174 |
| KUIP_108809 | *Scaphites hattini* | Kansas | Mitchell | Blue Hill | Heteromorph | 1.7856 |

| | | | | | | |
|---|---|---|---|---|---|---|
| SDSM_112533 | *Baculites rugosus* | Wyoming | | | Straight | 1.7852 |
| SDSM_112534 | *Placenticeras meeki* | Wyoming | | | Coiled | 1.7809 |
| SDSM_112535 | *Baculites grandis* | Wyoming | | | Straight | 1.828 |
| SDSM_112536 | *Baculites* | Wyoming | | | Straight | 1.795 |
| SDSM_112537 | *Baculites* | Wyoming | | | Straight | 1.8204 |
| SDSM_112538 | *Baculites* | Wyoming | | | Straight | 1.8112 |
| SDSM_112539 | *Baculites* | Wyoming | | | Straight | 1.7831 |
| SDSM_112540 | *Prionocyclus novimexicanus* | Wyoming | | | Coiled | 1.7985 |
| KUIP_143749 | *Scaphites carlilensis* | Kansas | Mitchell | Blue Hill | Heteromorph | 1.6214 |
| KUIP_143756 | *Prionocyclus hyatti* | Kansas | Osborne | Blue Hill | Coiled | 1.7729 |
| KUIP_143759 | *Prionocyclus hyatti* | Kansas | Osborne | Blue Hill | Coiled | 1.7724 |
| KUIP_148278 | *Placenticeras pseudoplacenta* | Kansas | Osborne | Blue Hill | Coiled | 1.7913 |
| KUIP_286636 | *Scaphites calilensis* | Kansas | Ellis | Blue Hill | Heteromorph | 1.7456 |
| KUIP_286656 | *Scaphites carlilensis* | Kansas | Ellis | Blue Hill | Heteromorph | 1.7422 |
| KUIP_312957 | *Scaphites carlilensis* | Kansas | Mitchell | Blue Hill | Heteromorph | 1.7414 |
| KUIP_312965 | *Scaphites carlilensis* | Kansas | Osborne | Blue Hill | Heteromorph | 1.6799 |
| KUIP_312971 | *Scaphites carlilensis* | Kansas | Osborne | Blue Hill | Heteromorph | 1.6899 |
| USGS_D10154 | *Baculites* | Texas | Fannin | | Straight | 1.5473 |
| USGS_D11410 | *Coilopoceras springeri* | New Mexico | Coffee | | Coiled | 1.7895 |
| USGS_D2387 | *Prionocyclus* | South Dakota | Butte | | Coiled | 1.6592 |
| USGS_D3743 | Ammonitida | South Dakota | | | Coiled | 1.7094 |
| DMNS_EPI.33630 | *Collignoniceras woolgari* | South Dakota | Fall River | | Coiled | 1.7331 |
| DMNS_EPI.33635 | *Scaphites nigricollensis* | South Dakota | Butte | | Heteromorph | 1.7829 |
| USGS_UN2 | *Baculites* | South Dakota | Butte | | Straight | 1.6905 |

# APPENDIX E

## Pierre Shale Complexity Data

| Museum # | Identification | State | County | Member | Shell Form | Complexity |
|---|---|---|---|---|---|---|
| KUIP_55 | Ammonitida | Wyoming | Upton | | Coiled | 1.7759 |
| KUIP_67 | Ammonitida | Wyoming | Upton | | Coiled | 1.7633 |
| KUIP_70 | *Baculites* | Wyoming | Upton | | Straight | 1.7596 |
| KUIP_91 | *Baculites* | Wyoming | Upton | | Straight | 1.77 |
| KUIP_92 | *Baculites* | Wyoming | Upton | | Straight | 1.7723 |
| KUIP_93 | *Baculites* | Wyoming | Upton | | Straight | 1.7904 |
| KUIP_206 | *Baculites* | Wyoming | Upton | | Straight | 1.6592 |
| KUIP_221 | Ammonitida | Wyoming | Upton | | Coiled | 1.7972 |
| KUIP_222 | Ammonitida | Wyoming | Upton | | Coiled | 1.7482 |
| KUIP_268 | *Baculites* | Wyoming | Upton | | Straight | 1.76 |
| KUIP_269 | *Baculites* | Wyoming | Upton | | Straight | 1.7612 |
| KUIP_273 | *Baculites* | Wyoming | Upton | | Straight | 1.6167 |
| KUIP_275 | *Baculites* | Wyoming | Upton | | Straight | 1.7889 |
| KUIP_276 | *Baculites* | Wyoming | Upton | | Straight | 1.7533 |
| KUIP_292 | *Baculites* | Wyoming | Upton | | Straight | 1.8049 |
| SDSM_304 | *Sphenodiscus lenticularis* | South Dakota | | | Coiled | 1.8215 |
| KUIP_313 | Ammonitida | Wyoming | Upton | | Coiled | 1.7983 |
| KUIP_320 | *Baculites* | Wyoming | Upton | | Straight | 1.7544 |
| KUIP_334 | *Baculites* | Wyoming | Upton | | Straight | 1.7546 |
| KUIP_340 | *Baculites* | Wyoming | Upton | | Straight | 1.7919 |
| KUIP_341 | *Baculites* | Wyoming | Upton | | Straight | 1.7891 |
| KUIP_347 | *Baculites* | Wyoming | Upton | | Straight | 1.7601 |
| KUIP_359 | Ammonitida | Wyoming | Upton | | Coiled | 1.6232 |
| KUIP_366 | *Baculites* | Wyoming | Upton | | Straight | 1.814 |
| KUIP_371 | *Baculites* | Wyoming | Upton | | Straight | 1.6966 |
| SDSM_392 | *Placenticeras meeki* | South Dakota | | | Coiled | 1.8175 |
| SDSM_396 | *Baculites compressus* | South Dakota | | | Straight | 1.721 |
| KUIP_396 | *Baculites* | Wyoming | Upton | | Straight | 1.8422 |
| FHSMIP_413 | *Baculites* | South Dakota | | | Straight | 1.789 |
| UCM_551 | Ammonitida | Colorado | Grand | | Coiled | 1.7887 |

| | | | | | | |
|---|---|---|---|---|---|---|
| FHSMIP_577 | *Placenticeras* | South Dakota | Pennington | | Coiled | 1.8192 |
| SDSM_862 | *Hoploscaphites nodosus* | South Dakota | | | Coiled | 1.7364 |
| FHSMIP_1076 | *Baculites* | Kansas | Wallace | Lake Creek | Straight | 1.6609 |
| FHSMIP_1267 | *Baculites grandis* | South Dakota | Meade | | Straight | 1.7997 |
| SDSM_1577 | *Baculites compressus* | South Dakota | | | Straight | 1.7205 |
| SDSM_1721 | *Anapachydiscus complexus* | South Dakota | | | Coiled | 1.7989 |
| UCM_2034 | *Heteroceras nebrascense* | Colorado | Larimer | | Heteromorph | 1.6885 |
| SDSM_2070 | Ammonitida | South Dakota | | | Coiled | 1.8346 |
| SDSM_2228 | *Baculites* | South Dakota | | | Straight | 1.684 |
| SDSM_2250 | *Baculites* | South Dakota | | | Straight | 1.7471 |
| UCM_2585 | *Baculites ovatus* | Wyoming | Albany | | Straight | 1.7421 |
| SDSM_2938 | *Didymoceras cheyennese* | South Dakota | | | Heteromorph | 1.7747 |
| SDSM_2948 | *Baculites* | South Dakota | | | Straight | 1.8062 |
| UCM_2966 | *Baculites ovatus* | Colorado | Larimer | | Straight | 1.7405 |
| SDSM_2968 | *Placenticeras* | South Dakota | Pennignton | | Coiled | 1.6942 |
| SDSM_2987 | *Baculites* | South Dakota | Hunter | | Straight | 1.8179 |
| SDSM_3014 | *Baculites* | South Dakota | | | Straight | 1.7773 |
| SDSM_3083 | *Placenticeras pseudocostatum* | South Dakota | Butte | | Coiled | 1.8333 |
| SDSM_3084 | Ammonitida | South Dakota | Butte | | Coiled | 1.7793 |
| UCM_3107 | *Baculites ovatus* | Colorado | Pueblo | | Straight | 1.7609 |
| SDSM_3283 | *Placenticeras* | South Dakota | Butte | | Coiled | 1.8188 |
| UCM_3853 | *Baculites ovatus* | Wyoming | Natrona | | Straight | 1.7761 |
| DMNS_4042 | *Placenticeras intercalare* | Colorado | Pueblo | | Coiled | 1.8121 |
| DMNS_4044 | *Placenticeras meeki* | Wyoming | Niobrara | | Coiled | 1.8208 |
| DMNS_4045 | *Placenticeras meeki* | Wyoming | Niobrara | | Coiled | 1.7773 |
| DMNS_4047 | *Placenticeras meeki* | Wyoming | Niobrara | | Coiled | 1.8151 |
| DMNS_4056 | *Menuites portlocki* | Wyoming | Niobrara | | Coiled | 1.7945 |
| DMNS_4068 | *Hoploscaphites* | Wyoming | Niobrara | | Coiled | 1.7958 |
| DMNS_4073 | *Discoscaphites* | Wyoming | Niobrara | | Coiled | 1.6894 |
| DMNS_4128 | *Baculites gilberti* | Wyoming | Niobrara | | Straight | 1.7122 |
| DMNS_4131 | *Baculites gregoryensis* | Colorado | Pueblo | | Straight | 1.718 |
| DMNS_4136 | *Baculites* | Wyoming | Niobrara | | Straight | 1.7736 |
| DMNS_4137 | *Baculites reesidei* | Wyoming | Niobrara | | Straight | 1.8393 |

| | | | | | | |
|---|---|---|---|---|---|---|
| DMNS_4138 | *Baculites compressus* | South Dakota | Pennington | | Straight | 1.7875 |
| DMNS_4139 | *Baculites perplexus* | Wyoming | Niobrara | | Straight | 1.7573 |
| DMNS_4140 | *Baculites scotti* | Wyoming | Niobrara | | Straight | 1.7683 |
| DMNS_4143 | *Baculites eliasi* | Wyoming | Niobrara | | Straight | 1.7727 |
| DMNS_4147 | *Baculites* | Montana | Carter | | Straight | 1.7955 |
| DMNS_4152 | *Baculites baculus* | South Dakota | Pennington | | Straight | 1.6803 |
| DMNS_4154 | *Baculites grandis* | Colorado | El Paso | | Straight | 1.7079 |
| UCM_4850 | *Baculites anceps* | Wyoming | Big Horn | | Straight | 1.7505 |
| DMNS_5633 | *Jeletzkytes nodosus* | Colorado | Larimer | | Coiled | 1.7736 |
| DMNS_7858 | *Baculites rugosus* | South Dakota | Pennington | | Straight | 1.7588 |
| DMNS_7867 | *Baculites reesidei* | South Dakota | Meade | | Straight | 1.7803 |
| DMNS_7871 | *Baculites grandis* | South Dakota | Pennington | | Straight | 1.7854 |
| UCM_8508 | *Baculites compressus* | Colorado | Elbet | | Straight | 1.7943 |
| DMNS_8718 | *Baculites* | Colorado | Pueblo | | Straight | 1.6959 |
| USGS_9161 | *Didymoceras jorgenseni* | South Dakota | Fall River | | Heteromorph | 1.7867 |
| UCM_9393 | *Heteroceras tortum* | Wyoming | Weston | | Heteromorph | 1.7536 |
| UCM_9395 | *Baculites ovatus* | Wyoming | Weston | | Straight | 1.8153 |
| UCM_9396 | *Baculites compressus* | Wyoming | Weston | | Straight | 1.778 |
| UCM_9798 | *Baculites compressus* | Colorado | Lincoln | | Straight | 1.754 |
| SDSM_10150 | *Placenticeras meeki* | South Dakota | | | Coiled | 1.7506 |
| SDSM_10169 | *Baculites* | South Dakota | | | Straight | 1.7454 |
| USGS_11725 | Ammonitida | Utah | Kane | | Coiled | 1.75 |
| UCM_13280 | *Placenticeras* | Wyoming | Albany | | Coiled | 1.7621 |
| UCM_15923 | *Placenticeras whitfieldi* | South Dakota | Pennington | | Coiled | 1.7787 |
| UCM_16878 | *Placenticeras whitfieldi* | South Dakota | Pennington | | Coiled | 1.8042 |
| DMNS_16889 | *Placenticeras costatum* | Colorado | Grand | | Coiled | 1.8012 |
| DMNS_16890 | *Placenticeras costatum* | Colorado | Grand | | Coiled | 1.8225 |
| DMNS_16898 | *Placenticeras costatum* | Colorado | Grand | | Coiled | 1.8179 |
| DMNS_16899 | *Placenticeras costatum* | Colorado | Grand | | Coiled | 1.795 |
| DMNS_16925 | *Placenticeras costatum* | Colorado | Grand | | Coiled | 1.8316 |
| DMNS_16926 | *Placenticeras costatum* | Colorado | Grand | | Coiled | 1.8047 |
| DMNS_16928 | *Placenticeras costatum* | Colorado | Grand | | Coiled | 1.8225 |

| | | | | | | |
|---|---|---|---|---|---|---|
| UCM_17316 | *Baculites ovatus* | Wyoming | Weston | | Straight | 1.7638 |
| UCM_17385 | *Scaphites nodasus* | Wyoming | Weston | | Heteromorph | 1.7631 |
| UCM_18483 | *Scaphites* | Wyoming | Weston | | Heteromorph | 1.7048 |
| UCM_18501 | *Baculites compressus* | Wyoming | Weston | | Straight | 1.7882 |
| UCM_19831 | *Baculites* | Wyoming | Niobrara | | Straight | 1.7168 |
| DMNS_19915 | *Baculites grandis* | Colorado | Jefferson | | Straight | 1.7798 |
| DMNS_19916 | *Baculites grandis* | Colorado | Jefferson | | Straight | 1.8235 |
| DMNS_19919 | *Jeletzkytes* | Colorado | Jefferson | | Coiled | 1.8129 |
| DMNS_19925 | *Baculites grandis* | Colorado | Jefferson | | Straight | 1.8003 |
| DMNS_19928 | *Jeletzkytes* | Colorado | Jefferson | | Coiled | 1.7739 |
| DMNS_19937 | *Baculites grandis* | Colorado | Jefferson | | Straight | 1.7657 |
| DMNS_19941 | *Baculites grandis* | Colorado | Jefferson | | Straight | 1.7672 |
| DMNS_19945 | *Jeletzkytes* | Colorado | Jefferson | | Coiled | 1.7255 |
| USGS_21422 | *Baculites sweetgrassensis* | Montana | Toole | | Straight | 1.7331 |
| USGS_22339 | *Metoicoceras whitei* | Utah | Kane | | Coiled | 1.7166 |
| DMNS_22877 | *Baculites grandis* | Colorado | Jefferson | | Straight | 1.767 |
| DMNS_22920 | *Baculites grandis* | Colorado | Jefferson | | Straight | 1.7544 |
| USGS_23056 | *Didymoceras cheyennsis* | Colorado | El Paso | | Heteromorph | 1.7332 |
| UCM_30222 | *Baculites* | Colorado | Grand | | Straight | 1.7643 |
| UCM_30392 | *Anapachydiscus* | Colorado | Pueblo | | Coiled | 1.798 |
| UCM_30394 | *Baculites scotti* | Colorado | Pueblo | | Straight | 1.7856 |
| DMNS_30421 | *Exiteloceras jenneyi* | Colorado | Larimer | | Heteromorph | 1.8084 |
| DMNS_30425 | *Baculites cunneatus* | Colorado | Larimer | | Straight | 1.7739 |
| DMNS_30431 | *Baculites grandis* | Colorado | Jefferson | | Straight | 1.7028 |
| DMNS_30433 | *Baculites grandis* | Colorado | Jefferson | | Straight | 1.8065 |
| UCM_31618 | *Baculites* | Colorado | Lincoln | | Straight | 1.7551 |
| UCM_32490 | *Placenticeras intercalare* | Colorado | Paso | | Coiled | 1.7913 |
| UCM_32492 | *Placenticeras intercalare* | Colorado | Paso | | Coiled | 1.7932 |
| UCM_32742 | *Placenticeras meeki* | Colorado | Grand | | Coiled | 1.7676 |
| KUIP_33986 | *Hoploscaphites nodosus* | Montana | Dawson | | Coiled | 1.6449 |
| KUIP_33990 | *Hoploscaphites nodosus* | Montana | Dawson | | Coiled | 1.7342 |
| KUIP_33991 | *Hoploscaphites nodosus* | Montana | Dawson | | Coiled | 1.7625 |
| KUIP_33993 | *Hoploscaphites nodosus* | Montana | Dawson | | Coiled | 1.7575 |

| | | | | | | |
|---|---|---|---|---|---|---|
| KUIP_34013 | *Hoploscaphites nodosus* | Montana | Dawson | | Coiled | 1.7221 |
| KUIP_34015 | *Hoploscaphites nodosus* | Montana | Dawson | | Coiled | 1.6729 |
| KUIP_34023 | *Hoploscaphites nodosus* | Montana | Dawson | | Coiled | 1.75 |
| KUIP_34066 | *Hoploscaphites nodosus* | Montana | Dawson | | Coiled | 1.7036 |
| KUIP_47172 | *Baculites* | Kansas | Wallace | Lake Creek | Straight | 1.7759 |
| KUIP_47186 | *Baculites reesidei* | Kansas | Wallace | Salt Grass Shale | Straight | 1.734 |
| KUIP_50108 | *Baculites* | Kansas | Wallace | | Straight | 1.7849 |
| KUIP_50121 | *Baculites* | Kansas | Logan | Sharon Springs | Straight | 1.7418 |
| KUIP_50143 | *Baculites* | Kansas | | Salt Grass Shale | Straight | 1.743 |
| KUIP_50163 | *Baculites* | Kansas | Cheyenne | Beecher Island | Straight | 1.7848 |
| KUIP_50164 | *Baculites corrugatus* | Kansas | Wallace | | Straight | 1.8069 |
| KUIP_50657 | *Baculites* | Kansas | | Beecher Island | Straight | 1.5656 |
| KUIP_50658 | *Baculites* | Kansas | | Beecher Island | Straight | 1.4813 |
| KUIP_50666 | *Baculites* | Colorado | | | Straight | 1.7664 |
| KUIP_50678 | *Baculites* | Colorado | | | Straight | 1.719 |
| KUIP_50679 | *Baculites* | Colorado | | | Straight | 1.7334 |
| KUIP_50685 | *Baculites ovatus* | Colorado | | | Straight | 1.753 |
| UT_53349 | *Placenticeras meeki* | South Dakota | Pennington | | Coiled | 1.6961 |
| KUIP_59646 | *Baculites reesidei* | Kansas | Wallace | | Straight | 1.7904 |
| KUIP_59647 | *Baculites reesidei* | Kansas | Wallace | | Straight | 1.7233 |
| KUIP_59661 | *Baculites pseudovatus* | Kansas | Wallace | | Straight | 1.7798 |
| KUIP_59662 | *Baculites reesodei* | Kansas | Wallace | | Straight | 1.7523 |
| KUIP_59665 | *Baculites grandis* | Kansas | Wallace | | Straight | 1.7609 |
| KUIP_59666 | *Baculites clinobatus* | Kansas | Wallace | | Straight | 1.7638 |
| KUIP_59667 | *Baculites grandis* | Kansas | Wallace | Beecher Island | Straight | 1.7139 |
| KUIP_59669 | *Baculites pseudovatus* | Kansas | Wallace | | Straight | 1.6623 |
| SDSM_64515 | *Baculites* | South Dakota | | | Straight | 1.8001 |
| SDSM_64531 | *Baculites* | South Dakota | | | Straight | 1.7463 |
| SDSM_68515 | *Baculites* | South Dakota | | | Straight | 1.7811 |
| USGS_88060 | *Baculites* | Colorado | Grand | | Straight | 1.807 |
| SDSM_109273 | *Pachydiscus* | South Dakota | | Red Bird | Coiled | 1.8183 |
| SDSM_109276 | *Placenticeras meeki* | South Dakota | | | Coiled | 1.7824 |

| | | | | | | |
|---|---|---|---|---|---|---|
| SDSM_109485 | *Baculites* | South Dakota | Pennington | | Straight | 1.7793 |
| SDSM_110491 | *Baculites* | South Dakota | | | Straight | 1.7372 |
| SDSM_112053 | *Prionocyclus* | South Dakota | | | Coiled | 1.7669 |
| SDSM_112530 | *Placenticeras meeki* | South Dakota | Butte | | Coiled | 1.8159 |
| SDSM_112531 | *Placenticeras meeki* | South Dakota | Butte | | Coiled | 1.7186 |
| SDSM_112532 | *Baculites* | South Dakota | Pennington | | Straight | 1.7401 |
| SDSM_112542 | *Pachydiscus* | South Dakota | | | Coiled | 1.7721 |
| SDSM_112600 | *Baculites* | South Dakota | | | Straight | 1.8295 |
| SDSM_112601 | *Baculites* | South Dakota | | | Straight | 1.7227 |
| SDSM_112602 | *Baculites* | South Dakota | | | Straight | 1.7877 |
| SDSM_112603 | *Baculites* | South Dakota | | | Straight | 1.8091 |
| SDSM_112604 | *Baculites* | South Dakota | | | Straight | 1.7344 |
| SDSM_112605 | *Baculites* | South Dakota | | | Straight | 1.717 |
| SDSM_112606 | *Baculites* | South Dakota | | | Straight | 1.7897 |
| SDSM_112607 | *Baculites* | South Dakota | | | Straight | 1.7859 |
| SDSM_113009 | *Placenticeras* | South Dakota | | | Coiled | 1.7941 |
| SDSM_113010 | *Placenticeras meeki* | South Dakota | | | Coiled | 1.7865 |
| SDSM_113011 | *Placenticeras* | South Dakota | | | Coiled | 1.8408 |
| SDSM_113013 | *Placenticeras meeki* | South Dakota | | | Coiled | 1.7892 |
| SDSM_113014 | *Placenticeras meeki* | South Dakota | | | Coiled | 1.8495 |
| SDSM_113015 | *Placenticeras meeki* | South Dakota | | | Coiled | 1.8166 |
| KUIP_148165 | *Hoploscaphites nodosus* | Montana | Dawson | | Coiled | 1.7693 |
| KUIP_148277 | *Placenticeras meeki* | Kansas | Wallace | Weskan | Coiled | 1.7935 |
| KUIP_148280 | *Placenticeras meeki* | Kansas | Wallace | Lake Creek | Coiled | 1.7919 |
| KUIP_148283 | *Placenticeras meeki* | Kansas | Wallace | Lake Creek | Coiled | 1.8019 |
| KUIP_148425 | *Baculites* | Colorado | Yuma | Beecher Island | Straight | 1.6888 |
| KUIP_150260 | *Hoploscaphites nodosus* | Montana | Dawson | | Coiled | 1.7684 |
| KUIP_150359 | *Baculites* | South Dakota | | | Straight | 1.7789 |
| KUIP_151185 | *Placenticeras* | Kansas | Wallace | Weskan | Coiled | 1.6871 |
| KUIP_297480 | *Placenticeras meeki* | Kansas | Wallace | Weskan | Coiled | 1.7218 |
| USGS_D13490 | *Didymoceras nebrascenses* | South Dakota | Fall River | | Heteromorph | 1.7896 |
| USGS_D1352 | *Baculites compressus* | Colorado | Grand | | Straight | 1.7077 |
| USGS_D1409 | *Didymoceras* | Colorado | Pueblo | | Heteromorph | 1.6254 |

| | | | | | | |
|---|---|---|---|---|---|---|
| USGS_D1411 | *Didymoceras* | Colorado | Pueblo | | Heteromorph | 1.6349 |
| USGS_D1422 | *Didymoceras nebrascenses* | South Dakota | Fall River | | Heteromorph | 1.7342 |
| USGS_D1467 | *Baculites* | Colorado | Larimer | | Straight | 1.7614 |
| USGS_D221 | *Didymoceras cheyennensis* | Colorado | El Paso | | Heteromorph | 1.7031 |
| USGS_D2629 | *Didymoceras nebrascenses* | South Dakota | Fall River | | Heteromorph | 1.7042 |
| USGS_D2719 | *Baculites reesidei* | Colorado | Larimer | | Straight | 1.7682 |
| USGS_D2821 | *Baculites reesidei* | Colorado | Larimer | | Straight | 1.7911 |
| USGS_D368 | *Baculites* | Colorado | Larimer | | Straight | 1.7418 |
| USGS_D409-1 | *Didymoceras tortum* | South Dakota | Buffalo | | Heteromorph | 1.6441 |
| USGS_D409-2 | *Didymoceras cochleatum* | South Dakota | Buffalo | | Heteromorph | 1.6824 |
| USGS_D409-3 | *Didymoceras platycostatum* | South Dakota | Buffalo | | Heteromorph | 1.6835 |
| USGS_D409-4 | *Didymoceras mortoni* | South Dakota | Buffalo | | Heteromorph | 1.7565 |
| USGS_D5033 | *Baculites* | Colorado | Larimer | | Straight | 1.8014 |
| USGS_D5416 | *Baculites compressus* | Colorado | Grand | | Straight | 1.7864 |
| USGS_D5974 | *Baculites scotti* | Colorado | Grand | | Straight | 1.695 |
| USGS_D8771 | *Didymoceras cheyennensis* | Colorado | El Paso | | Heteromorph | 1.6728 |
| USGS_D904 | *Didymoceras* | Colorado | Pueblo | | Heteromorph | 1.7348 |
| DMNS_EPI.16893 | *Placenticeras costatum* | Colorado | Grand | | Coiled | 1.7893 |
| DMNS_EPI.33138 | *Placenticeras cummungsi* | New Mexico | Rattlesnake | Colorado | Coiled | 1.8147 |
| DMNS_EPI.33140 | *Pseudaspidoceras pseudonodosoides* | New Mexico | Rattlesnake | Colorado | Coiled | 1.8268 |
| DMNS_EPI.33384 | *Jeletzkytes criptonodosus* | Wyoming | Niobrara | | Coiled | 1.8289 |
| DMNS_EPI.33387 | *Menuites oralensis* | Wyoming | Niobrara | | Coiled | 1.8134 |
| DMNS_EPI.33390 | *Jeletzkytes criptonodosus* | Wyoming | Niobrara | | Coiled | 1.7006 |
| DMNS_EPI.33391 | *Jeletzkytes plenus* | Wyoming | Niobrara | | Coiled | 1.7615 |
| DMNS_EPI.33396 | *Jeletzkytes plenus* | Wyoming | Niobrara | | Coiled | 1.7687 |
| DMNS_EPI.33411 | *Placenticeras meeki* | Wyoming | Niobrara | | Coiled | 1.7576 |
| DMNS_EPI.33413 | *Placenticeras intercalare* | Wyoming | Niobrara | | Coiled | 1.7599 |
| DMNS_EPI.33417 | *Jeletzkytes criptonodosus* | Wyoming | Weston | | Coiled | 1.7701 |
| DMNS_EPI.33421 | *Jeletzkytes criptonodosus* | Wyoming | Niobrara | | Coiled | 1.6471 |
| DMNS_EPI.33426 | *Hoploscaphites* | Wyoming | Niobrara | | Coiled | 1.6196 |
| DMNS_EPI.33427 | *Hoploscaphites* | Wyoming | Niobrara | | Coiled | 1.8242 |

| | | | | | | |
|---|---|---|---|---|---|---|
| DMNS_EPI.33433 | *Menuites portlocki complexus* | Wyoming | Niobrara | | Coiled | 1.7989 |
| DMNS_EPI.33439 | *Menuites oralensis* | Wyoming | Niobrara | | Coiled | 1.8215 |
| DMNS_EPI.33618 | *Jeletzkytes brevis* | South Dakota | Pennington | | Coiled | 1.7156 |
| DMNS_EPI.33628 | *Scaphites carlensis* | South Dakota | Butte | | Heteromorph | 1.771 |
| DMNS_EPI.33631 | *Menuites oralensis* | South Dakota | Fall River | | Coiled | 1.7375 |
| DMNS_EPI.33636 | *Prionocyclus* | South Dakota | Fall River | | Coiled | 1.7331 |
| DMNS_EPI.33637 | *Jeletzkytes nodosus* | South Dakota | Pennington | | Coiled | 1.7131 |
| DMNS_EPI.33638 | *Jeletzkytes* | South Dakota | Pennington | | Coiled | 1.7632 |
| DMNS_EPI.36401 | *Placenticeras meeki* | Colorado | Fremont | | Coiled | 1.6814 |
| DMNS_EPI.36403 | *Exiteloceras jenneyi* | Colorado | Pueblo | | Heteromorph | 1.7531 |
| DMNS_EPI.36406 | *Didymoceras stevensoni* | Colorado | Larimer | | Heteromorph | 1.6372 |
| DMNS_EPI.36411 | *Placenticeras meeki* | Colorado | Larimer | | Coiled | 1.8258 |
| DMNS_EPI.36426 | *Placenticeras meeki* | Colorado | Pueblo | | Coiled | 1.7734 |
| DMNS_EPI.36427 | *Metoicoceras* | Colorado | Pueblo | | Coiled | 1.7714 |
| DMNS_EPI.36429 | *Menuites oralensis* | Colorado | Pueblo | | Coiled | 1.7842 |
| DMNS_EPI.36439 | *Rhaeboceras halli* | Colorado | Larimer | | Coiled | 1.8007 |
| DMNS_EPI.36443 | *Placenticeras costatum* | Colorado | Boulder | | Coiled | 1.8356 |
| DMNS_EPI.36448 | *Placenticeras placenta* | Colorado | Jefferson | | Coiled | 1.7732 |
| DMNS_EPI.36452 | *Scaphites tetonensis* | Montana | Chouteau | Colorado | Heteromorph | 1.7237 |
| DMNS_EPI.36458 | *Jeletzkytes quadrangularis* | Montana | Dawson | | Coiled | 1.8111 |
| DMNS_EPI.36460 | *Jeletzkytes crassus* | Montana | Dawson | | Coiled | 1.7585 |
| DMNS_EPI.36462 | *Jeletzkytes crassus* | Montana | Dawson | | Coiled | 1.7119 |
| DMNS_EPI.36465 | *Jeletzkytes plenus* | Montana | Dawson | | Coiled | 1.7275 |
| DMNS_EPI.36466 | *Jeletzkytes brevis* | Montana | Dawson | | Coiled | 1.7795 |
| DMNS_EPI.36468 | *Jeletzkytes nodosus* | Montana | Dawson | | Coiled | 1.7368 |
| DMNS_EPI.36471 | *Placenticeras intercolari* | Montana | Carter | | Coiled | 1.7583 |
| DMNS_EPI.36475 | *Scaphites preventricosus* | Montana | Toole | Colorado | Heteromorph | 1.7734 |
| DMNS_EPI.36478 | *Clioscaphites novimexicanus* | Montana | Toole | Colorado | Coiled | 1.7867 |
| DMNS_EPI.36490 | *Baculites compresssus* | Wyoming | Niobrara | | Straight | 1.7119 |
| DMNS_EPI.36769 | *Baculites eliasi* | Wyoming | Niobrara | | Straight | 1.7632 |
| DMNS_EPI.36782 | *Baculites* | Montana | Carter | | Straight | 1.7478 |

| | | | | | | |
|---|---|---|---|---|---|---|
| DMNS_EPI.36786 | *Baculites* | Montana | Carter | | Straight | 1.6247 |
| DMNS_EPI.4181 | *Baculites eliasi* | Wyoming | Niobrara | | Straight | 1.7694 |
| DMNS_EPI.547 | *Scaphites plenus* | South Dakota | | | Heteromorph | 1.7538 |